Demonstration of a self-healing all-polymer distributed Bragg reflector laser

Yunli Lu,[1] Zoe Lowther,[1] Nicholas D. Christianson,[1] Zhenpeng Li,[2] Eric Baer,[2] Mark G. Kuzyk,[3] and Nathan J. Dawson[1, 3, 4, a)]

[1)]*Department of Natural Sciences, Hawaii Pacific University, Kaneohe, HI 96744, USA*

[2)]*Department of Macromolecular Science and Engineering, Case Western Reserve University, Cleveland, OH 44106, USA*

[3)]*Department of Physics and Astronomy, Washington State University, Pullman, WA 99164, USA*

[4)]*Department of Computer Science and Engineering, Hawaii Pacific University, Honolulu, HI 96813, USA*

(Dated: 8 February 2020)

Self-healing of an all-polymer distributed Bragg reflector laser is demonstrated. The lasing medium is a glycol-modified poly(ethylene terephthalate) co-polymer doped with rhodamine 6g. After the light output is reduced to $1/3$ of its pristine value through photodegradation due to the pump, the laser is placed in the dark to allow it to heal. The laser fully recovered to its pre-damaged output power. A similar laser made with the rhodamine B chromophore is observed to only partially recover after photodegradation.

The advantage of a dye laser's high gain and broad range of tunability is offset by the common problem of gain loss due to photodegradation induced by the pump. The lifetime of a dye laser is commonly extended by using a liquid solution reservoir which is cycled through a dye laser cell,[1] thus replacing the photodegraded chromophores. However, liquid lasers can not be miniaturized given the requirement of a large reservoir of chromophores, and they require cleaning and changing dyes often which can be messy. The reservoir design does not reduce the rate at which the chromophores degrade, but simply increases the number of available dye molecules, leading to a significant amount of waste material.

Solid-state lasers can be miniaturized for applications that require small coherent light sources such as microlasers used in the medical field[2,3] and integrated photonics.[4–6] Organic solid-state lasers have been developed using several cost-effective methods[7–11] for applications that require broad tunability.[12–14] Here we use all-polymer, multilayer, distributed Bragg reflector (DBR) lasers that are fabricated by piecing together an extruded plastic multilayer sheet with a thin dye-doped polymer film.[15,16]

The gain medium of solid-state organic dye lasers is subject to photodegradation, which is a considerable disadvantage.[17] Some of the most efficient laser dyes are short-lived,[18] which can result in short lifetimes in the solid-state. When doped into certain polymer matrices, some photobleachable chromophores have been observed to either partially or fully recover their optical properties.[19–30] Thermodynamic statistical models have been introduced to explain much of the self-healing phenomena observed for anthraquinone derivatives doped in poly(methyl methacrylate).[31,32] The first self-healing organic-inorganic hybrid lasers were illustrated by Anderson et al. using a random laser architecture with inorganic nanoparticles dispersed in a dye-doped polymer matrix.[33–35] Photobleached rhodamine 6g (R6g) in a glycol-modified poly(ethylene terephthalate) co-polymer (PETG) was observed to recover its amplified spontaneous emission (ASE) after being in the dark.[36] A spectral shift in the recovered R6g gain profile was observed in the polyurethane (PU) matrix caused by photocleavage and oxidation of the polymer followed by aggregation of R6g,[35] whereas the recovered R6g gain profile in PETG showed remarkable spectral stability.[36] This paper demonstrates a self-healing all-polymer DBR laser made with a R6g-PETG gain medium. We discuss how such lasers are fabricated and characterized.

The DBR laser is made from a gain medium sandwiched between two polymer Bragg mirrors. The multilayer polymer Bragg reflectors are fabricated via a co-extrusion process.[37] Each reflector has 256 layers that alternate between the high refractive index polymer polystyrene (PS) and the low refractive index polymer poly(methyl methacrylate) (PMMA). The multilayer reflectors are co-extruded with two low-density polyethylene skin layers on each side, which are removed before the gain medium is placed between them.

The gain medium layer is fabricated as follows. Rhodamine 6g (R6G per chlorate purchased from Sigma-Aldrich) and PETG (purchased from 3DXTech) in the ratio of 1 wt.% is added to chloroform at a ratio of 15 wt.% solids in a capped silica borate container. The chemical structure of the dye and polymer are shown in Figure 1(c). The mixture is sonicated for one hour at a temperature of 60 °C. Because the Bragg reflectors are made from alternating layers of PMMA and PS, which both rapidly dissolve in chloroform, the gain medium must be a freestanding film during the fabrication process.

A thin layer of poly(vinyl alcohol) (PVOH) (purchased from Polyscience) is spin coated onto 1"×1" squares of precut glass microscope slides at 3000 rpm for 30 seconds from a 4 wt.% solution in deionized (DI) water. The PVOH layer rests for 5 minutes before spin coating a thick R6g-PETG layer from solution at 1450 rpm for 3 seconds over the PVOH. The sample is allowed to rest for 10 minutes, and then annealed in an oven for another 10 minutes at 140 °C. The glass slide coated with the bilayer is sonicated in a bath of DI wa-

a)Electronic mail: ndawson@hpu.edu

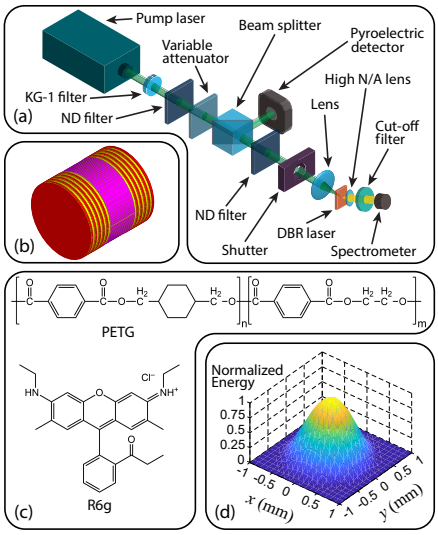

FIG. 1. (a) A diagram of the self-healing DBR laser experiment and (b) a cartoon of a circular section of the DBR laser, where there are actually 256 layers on each Bragg reflector surrounding the gain medium. (c) The chemical structures of the host polymer and dopant chromophore. (d) The pump beam profile incident on the surface of the DBR laser at an incident angle of 25° with respect to the surface normal.

ter until the PVOH is completely dissolved and a freestanding R6g-doped PETG monolayer floats to the surface of the bath.

The DBR laser is made as follows. A 1 cm×1 cm square is cut from the center of the R6g-doped PETG film. A nominal 1 cm ×2 cm sheet of PS/PMMA is coated in a thin layer of PVOH and the gain layer is placed onto one side of the reflector. The multilayer sheet is then folded over the gain layer and held under pressure for three days. The crease of the fold is perpendicular to the extrusion direction. A diagram showing a circular cross-section of the gain layer and first few layers of the Bragg reflector is shown in Figure 1(b).

The reflection band of the multilayer film is heterogeneous throughout the area of the multilayer film due to layer thickness gradients. Therefore, the pump beam is focused onto a small spot. The fluorescence from a low intensity pump beam is imaged onto a CMOS detector, where the intensity profile of the pump beam is shown in Figure 1(d). A spot radius of $\sim 500\,\mu$m is estimated from the nearly concentric circle formed around a $1/e$ amplitude of the normalized intensity profile. The pump intensity is increased above the DBR threshold for the self-healing experiment. The layer thickness gradients are significantly smaller along the extrusion direction. Thus, folding the multilayer film with a crease in the direction perpendicular to the extrusion direction when sandwiching the gain medium results in a set of mirrors with greater symmetry relative to a folded multilayer with a crease parallel to the extrusion direction. The pump beam is directed toward a location on the DBR laser where the reflection band of the polymer Bragg mirrors are centered near 600 nm. Lasing consistently occurs at the long-wavelength band edge, which has a low group velocity due to the large dispersion at the band edge.

The 532 nm wavelength pump beam is generated from frequency doubling a $1.064\,\mu$m laser of 6 ns pulse width and 10 Hz repetition rate. The pump beam initially passes through a KG-1 filter to remove the residual $1.064\,\mu$m light as shown in Figure 1(a). The 532 nm light is attenuated via a 2 O.D neutral density filter followed by a variable neutral density filter attached to a linear actuator. The beam is then split with one beam incident on an Ophir PE10-C pyroelectric detector.

Because the self-healing experiment runs for over an hour, pump beam drift is compensated for with an actuator that adjusts the variable attenuator in response to changes of the pump power. Compensation kicks in when the average energy over 50 pulses varies by more than 1.2%. After the pump passes through the beam splitter, it is further reduced by a 1 O.D. neutral density filter. The pump beam continues to a shutter, which is controlled by a relay. The relay opens the shutter at the beginning of each degradation experiment. The shutter automatically closes when the photodegraded DBR laser light is measured to be $\leq 32\%$ of the initially measured output energy. The automated recovery experiment follows the degradation experiment, where the shutter is opened for short time intervals to monitor recovery of the DBR laser's output energy.

After the pump beam passes through the shutter, it is focused onto the DBR laser at an incident angle of 25° from the normal direction. The DBR laser output is captured by a high numerical aperture (NA) lens and directed through a 550 nm long-pass filter to remove any residual 532 nm light scattered from the sample. The DBR laser light is finally directed to an optical fiber leading to an Ocean Optics USB4000 spectrometer with a 100 ms integration time. The variable attenuator attached to a linear actuator, pyroelectric detector, shutter, and spectrometer are all connected to a single computer that automates the self-healing experiment.

The pump beam's light is absorbed by the R6g chromophore, some of which is emitted as fluorescence. The cavity formed by the Bragg reflectors sandwiching the gain medium induces lasing when the pump power is increased above threshold. The energy per pulse of the pump beam incident on the surface of the DBR laser is $8\,\mu$J for the duration of the self-healing laser experiment. The emission spectra for the pristine, degraded, and recovered samples are shown in the inset of Figure 2. The emission intensity from the pristine sample is normalized to unity at the beginning of the experiment.

The emitted intensity is a nonlinear function of the chromophore population density which can be expanded as a Taylor series about the initial population density, $I(N) = (N - N_0)dI/dN|_{N=N_0} + [(N - N_0)^2/2]d^2I/dN^2|_{N=N_0} + \cdots$. For small changes in concentration, a linear approximation can be made, $I(N) \approx (N - N_0)dI/dN|_{N=N_0}$, where the constant of proportionality is directly related to the photodegradation and

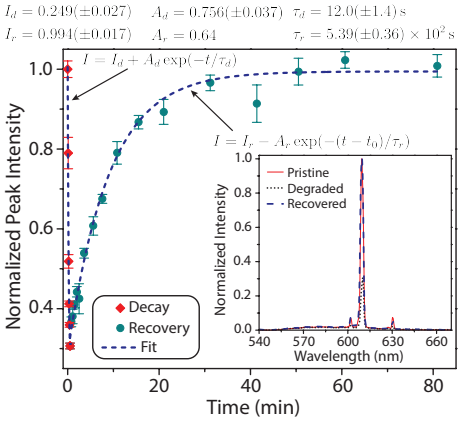

FIG. 2. The photodegradation (diamonds), recovery (circles) and exponential fit (dashed curve) of an all-polymer DBR laser with a R6g-doped PETG gain medium. The inset shows the emission spectra for the pristine, photodegraded, and recovered DBR laser.

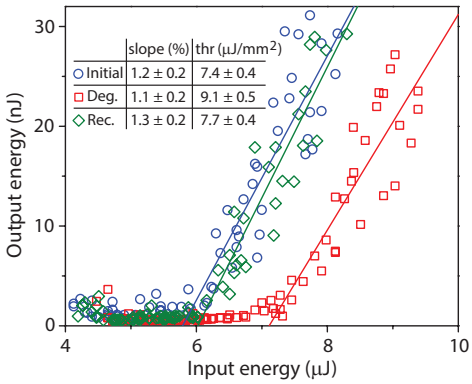

FIG. 3. The initial (circles), degraded (squares), and recovered (diamonds) J-curves for the DBR laser with a R6g-doped PETG gain medium. The slope efficiency and thresholds are tabulated to the left of the plotted data.

recovery rate. The fluorescence intensity is a linear function of the dye concentration in the absence of aggregation. In a DBR laser, $I(N)$ is a nonlinear function and the time constants for degradation/recovery are shorter because $N_0 \gg 0$ for laser emission.

The decay data, which is collected at 10 s intervals, is fit to the solution of the linear rate equation solution $I = I_d + A_d \exp(-t/\tau_d)$ – shown in Figure 2 – yielding a decay time constant of $\tau_d = 12.0(\pm 1.4)$ s and leveling off to the steady state emission of $I_d = 0.249(\pm 0.027)$ at $t \to \infty$.

After the measured DBR laser output drops below 32% of the initial energy per pulse, the shutter is closed to start the self healing process. The shutter is opened sparingly for brief moments to collect recovery data while the sample is otherwise in the dark. Each data point in Figure 2 represents an average of six pulses. The short duration of pumping minimizes the amount of photodegradation while the chromophores recover in the dark. The uncertainties are estimated from the corrected standard deviation.

The recovery data is shown in Figure 2 with blue circles. A fit of the data to the exponential growth function $I = I_r - A_r \exp[-(t - t_{sh})/\tau_r]$ yields a recovery time constant $\tau_r = 5.39(\pm 0.36) \times 10^2$ s, or about 9 minutes, and amplitude $I_r = 0.994(\pm 0.017)$, corresponding to full recovery within experimental uncertainty. Thus, the dominant photodegradation pathways of R6g are reversible when doped in PETG, where the probability of an R6g chromophore in a PETG matrix undergoing an irreversible photodegradation process appears to be negligible.

Another interesting outcome of using PETG as a host polymer is the photostability of the device output spectrum. There is no significant change in the emission spectrum as observed in the inset of Figure 2. Because the lasing wavelength is pinned to the reflection band edge of the DBR laser, there should be no measurable change in the operating wavelength, even when there are irreversible changes in the host polymer. Previous results from ASE studies showed that the gain envelope of an R6g-doped PETG monolith is stable throughout the photodegradation and recovery process.[36] Thus, because there were no significant changes in the gain envelope profile or operating wavelength, the peak intensity of the recovered DBR laser can indeed be directly compared to the peak intensity of the pristine laser. Thus, full recovery of the laser intensity, within uncertainty, is directly correlated to full recovery of the chromophores in the gain medium.

After the DBR laser fully recovered over one cycle, the experiment is repeated to get J-curve data. The variable attenuator is slowly translated to reduce the power immediately after the shutter is opened at the beginning of the experiment. Single shot data is collected by the reference detector and spectrometer while the power is slowly reduced. The variable attenuator is moved to its original position after each J-curve data run. For the J-curve of the photodegraded DBR laser, the attenuator is quickly moved so that the pump power increases to account for the drop in the DBR laser's emission; the attenuator is then slowly translated to reduce the pump power. After the experiment, an Ophir PE10-C detector is placed in front of the DBR laser to relate the reference energy to the pump energy incident on the surface of the DBR laser. An Ophir PE9-C-ES detector and a neutral density filter is used to relate the DBR laser beam's peak intensity measured by the spectrometer to the absolute energy per pulse, where losses from reflections at the high NA lens and long-pass filter interfaces were included in the calibration.

Three sets of data are recorded during the second experiment: 1) initial, 2) degraded, and 3) recovered J-curves. The three sets of data are shown in Figure 3 with tabulated thresholds and slope efficiencies. The slope efficiencies for the ini-

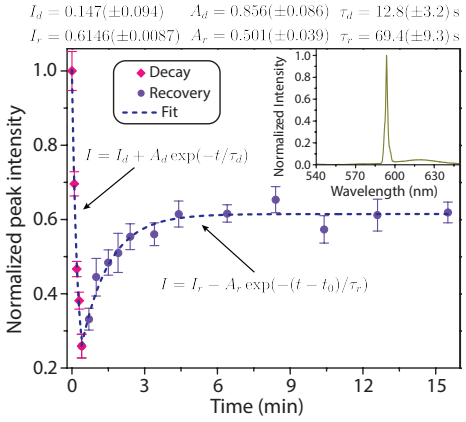

FIG. 4. Photodegradation of a DBR laser with a RhB-doped PETG gain medium followed by recovery as probed by an interment pump while otherwise being left in the dark. The inset shows the emission spectrum of the pristine DBR laser.

tial, degraded, and recovered J-curves are all within uncertainty. The DBR laser threshold increased significantly for the photodegraded gain medium. The slope efficiencies and thresholds for the initial and recovered states are equal within experimental uncertainty determined from the linear fits.

A second DBR laser with a different rhodamine derivative was fabricated to check the novelty of the recoverable R6g-PETG gain medium used in the self-healing DBR lasers. The second DBR laser's gain medium used the same PETG matrix, but the dopant molecule was rhodamine B (RhB). The ratio of dye to polymer was nominally 1 wt.%. The solvent processing and fabrication procedures were similar to those provided for the DBR laser with the R6g-PETG gain medium. The DBR laser with the RhB-doped PETG gain medium had a higher threshold, and it was pumped with an energy of $14\,\mu$J per pulse. The results for photodegradation and recovery in the dark are shown in Figure 4 with an inset that shows the initial emission spectrum captured by the spectrometer.

The decay time constant was found to be $\tau_d = 12.8(\pm 3.2)$ s and leveling off to the steady state emission at infinite time of $I_d = 0.147(\pm 0.094)$. The recovery data is shown in Figure 4 with violet circles. A fit of the data to the exponential growth function yields a recovery time constant $\tau_r = 69.4(\pm 9.3)$ s, or just over a minute, and amplitude $I_r = 0.6146(\pm 0.0087)$ corresponding to partial recovery. Therefore, a substantial amount of irreversible photodegradation is also observed. Partial recovery of the fluorescence signal of RhB-doped PMMA was previously observed by Peng et al.,[19] which is consistent with our findings for the DBR laser with a RhB-PETG gain medium. Both PMMA and PETG contain repeating ester groups, which likely play a role in the recovery of some chromophores when in a polymer host.[36]

The photodegradation time constant τ_d and steady state undegraded population N_u, which lases, depends on the intensity. As shown by Zhu,[24] τ_d and N_u depend on the pump intensity I_p according to

$$\tau_d = \left(\frac{1}{\tau_r} + \alpha I_p\right)^{-1} \quad \text{and} \quad N_u = \frac{1}{\tau_r}\left(\frac{1}{\tau_r} + \alpha I_p\right)^{-1}, \quad (1)$$

where α defines an intrinsic photodegradation rate. Indeed, we observe that the degradation rate increases with increased pump intensity and that the steady state intensity, as determined from the population of lasing chromophores, decreases according to Equations 1.

Solving for the photodegradation parameter α using Equation 1 gives $\alpha = (1/\tau_d - 1/\tau_r)/I_p$. Assuming that the pump intensity is proportional to the energy per pulse, the degradation parameter of the RhB medium is about 0.4 times that of the R6g medium. Given the rather large uncertainty in determining the intensity of pump light that reaches the lasing medium, the degradation parameters are within experimental uncertainty of being approximately equal; but, one material fully recovers and the other does not which shows that the chemical composition is an important factor in self healing.

We have demonstrated that some materials can be used to make self-healing Bragg grating polymer lasers. With further material improvements, it may be possible to make reliable organic lasers that recover after photodegradation. More importantly, the laser might run in its steady state, where photodegradation is balanced by healing for longer periods of time than more robust materials that do not recover; however, we must stress that photodegradation and self healing is a complex problem that involves both the material and geometry of the laser. For example, Anderson et. al. observed that both the peak position and width of the random laser varies during a cycle, and explained this in terms of the formation of dimers and trimers.[33–35] We did not observe such shifts, but our power levels are different. Past studies have shown stability and short-time healing of photobleached R6G-doped PVOH attributed to recovery from a triplet state and another *a priori* dark state[20] which has been hypothesized as an anion doublet state.[38] These short-time-scale recoverable states observed in R6g can also be converted to irreversible photobleached states when R6g is doped in PVOH.[38] Negligible recovery of photobleached R6g has been observed over long time scales when doped in highly hydrolyzed PVOH;[36] however, large-scale recovery R6g emission has been observed when doped in PU and PETG over long times.[34–36] Classical diffusion of the dye in its thermoplastic host is not responsible for the long-time-scale recovery from a photobleached state,[25] and the healing appears to occur in polymers with repeating ester groups making the self-healing phenomenon observed in this study to be a chemical process involving both the dye and matrix.[27,36] While much light has been shed on the healing process, the mechanisms are not well understood and require more study. All of these properties need to be brought together into one coherent theory if the underlying mechanisms are to be fully elucidated.

The importance of the dopant is illustrated by the fact that a DBR laser made with a R6g-PETG gain medium heals while

a DBR laser made with a RhB-PETG gain medium only partially heals. The stability of the gain envelope of the R6g-doped PETG material and the static emission characteristics of the passive cavity make the DBR laser with the R6g-PETG gain medium a useful benchmark for self-healing organic lasers. Laser architectures with low thresholds could significantly lower the photodegradation rate and allow for higher repetition rate devices. Altering the passive cavity design to also increase the slope efficiency could fulfill applications requiring tunable solid-state microcavity lasers that can deliver a higher power output emission with low thresholds. Further materials studies are required to identify the mechanisms of self healing so that better lasing media can be developed.

ACKNOWLEDGMENTS

NJD thanks the Hawaii Pacific University, CNCS Scholarly Endeavors Program for supporting this work. ZL thanks the National Science Foundation, Louis Stokes Alliances for Minority Participation, #HRD 1826864.

[1] F. Duarte and L. W. Hillman, *Dye laser principles, with applications* (Academic Press, Boston, 1987).
[2] J. Mysliwiec, K. Cyprych, L. Sznitko, and A. Miniewicz, "Biomaterials in light amplification," J. Opt. **19**, 033003 (2017).
[3] M. Manzo and R. Schwend, "A Novel Microlaser-Based Plasmonic-Polymer Hybrid Resonator for Multiplexed Biosensing Applications," J. Eng. Sci. Med. Diagn. Ther. **2** (2019).
[4] M. M. Karow, P. Munnelly, T. Heindel, M. Kamp, S. Höfling, C. Schneider, and S. Reitzenstein, "On-chip light detection using monolithically integrated quantum dot micropillars," Appl. Phys. Lett. **108**, 081110 (2016).
[5] W. Zhang, J. Yao, and Y. S. Zhao, "Organic Micro/Nanoscale Lasers," Acc. Chem. Res. **49**, 1691–1700 (2016).
[6] F. Tabataba-Vakili, L. Doyennette, C. Brimont, T. Guillet, S. Rennesson, E. Frayssinet, B. Damilano, J.-Y. Duboz, F. Semond, I. Roland, M. El Kurdi, X. Checoury, S. Sauvage, B. Gayral, and P. Boucaud, "Blue Microlasers Integrated on a Photonic Platform on Silicon," ACS Photon. **5**, 3643–3648 (2018).
[7] T. Komikado, S. Yoshida, and S. Umegaki, "Surface-emitting distributed-feedback dye laser of a polymeric multilayer fabricated by spin coating," Appl. Phys. Lett. **89**, 061123 (2006).
[8] K. D. Singer, T. Kazmierczak, J. Lott, H. Song, Y. Wu, J. Andrews, E. Baer, A. Hiltner, and C. Weder, "Melt-processed all-polymer distributed bragg reflector laser," Opt. Express **16**, 10358–10363 (2008).
[9] G. Canazza, F. Scotognella, G. Lanzani, S. De Silvestri, M. Zavelani-Rossi, and D. Comoretto, "Lasing from all-polymer microcavities," Laser Phys. Lett. **11**, 035804 (2014).
[10] O. Mhibik, S. Chénais, S. Forget, C. Defranoux, and S. Sanaur, "Inkjet-printed vertically emitting solid-state organic lasers," J. Appl. Phys. **119**, 173101 (2016).
[11] A. Sarkar, R. Venkataraj, V. P. N. Nampoori, and M. Kailasnath, "Silver nanoparticles filled hollow polymer fiber laser with enhanced photostability," Opt. Laser Technol. **112**, 255–260 (2019).
[12] G. Mao, J. Andrews, M. Crescimanno, K. D. Singer, E. Baer, A. Hiltner, H. Song, and B. Shakya, "Co-extruded mechanically tunable multilayer elastomer laser," Opt. Mater. Express **1**, 108–114 (2011).
[13] J. H. Andrews, M. Crescimanno, N. J. Dawson, G. Mao, J. B. Petrus, K. D. Singer, E. Baer, and H. Song, "Folding flexible co-extruded all-polymer multilayer distributed feedback films to control lasing," Opt. Express **20**, 15580–15588 (2012).
[14] Y. Feng, X. Yu, R. Zhang, J. Wu, P. Zhang, S. Chen, and D. Zhang, "Continuously tunable organic solid-state laser based on the adjustment of effective refractive index," J. Alloys Compd. **729**, 513–517 (2017).
[15] J. H. Andrews, M. Aviles, M. Crescimanno, N. J. Dawson, A. Mazzocco, J. B. Petrus, K. D. Singer, E. Baer, and H. Song, "Thermo-spectral study of all-polymer multilayer lasers," Opt. Mater. Express **3**, 1152–1160 (2013).
[16] J. H. Andrews, M. Crescimanno, K. D. Singer, and E. Baer, "Melt-processed polymer multilayer distributed feedback lasers: Progress and prospects," J. Polym. Sci. B **52**, 251–271 (2014).
[17] E. Ippen, C. Shank, and A. Dienes, "Rapid photobleaching of organic laser dyes in continuously operated devices," IEEE J. Quant. Electron. **7**, 178–179 (1971).
[18] I. P. Kaminow, L. W. Stulz, E. A. Chandross, and C. A. Pryde, "Photobleaching of Organic Laser Dyes in Solid Matrices," Appl. Opt. **11**, 1563–1567 (1972).
[19] G. D. Peng, Z. Xiong, and P. L. Chu, "Fluorescence decay and recovery in organic dye-doped polymer optical fibers," J. Lightwave Technol. **16**, 2365 (1998).
[20] R. Zondervan, F. Kulzer, S. B. Orlinskii, and M. Orrit, "Photoblinking of Rhodamine 6G in Poly(vinyl alchohol): Radical Dark State Formed through the Triplet," J. Phys. Chem. A **107**, 6770–6776 (2003).
[21] B. F. Howell and M. G. Kuzyk, "Lasing action and photodegradation of disperse orange 11 dye in liquid solution," Appl. Phys. Lett. **85**, 1901–1903 (2004).
[22] P. Kobrin, R. Fisher, and A. Gurrola, "Reversible photodegradation of organic light-emitting diodes," Applied Physics Letters **85**, 2385–2387 (2004).
[23] N. Tanaka, N. Barashkov, J. Heath, and W. N. Sisk, "Photodegradation of polymer-dispersed perylene di-imide dyes," Appl. Opt. **45**, 3846–3851 (2006).
[24] Y. Zhu, J. Zhou, and M. G. Kuzyk, "Two-photon fluorescence measurements of reversible photodegradation in a dye-doped polymer," Opt. Lett. **32**, 958–960 (2007).
[25] S. K. Ramini, N. Dawson, and M. G. Kuzyk, "Testing the diffusion hypothesis as a mechanism of self-healing in disperse orange 11 doped in poly(methyl methacrylate)," J. Opt. Soc. Am. B **28**, 2408–2412 (2011).
[26] B. R. Anderson, S.-T. Hung, and M. G. Kuzyk, "Wavelength dependence of reversible photodegradation of disperse orange 11 dye-doped pmma thin films," J. Opt. Soc. Am. B **32**, 1043–1049 (2015).
[27] S.-T. Hung, A. Bhuyan, K. Schademan, J. Steverlynck, M. D. McCluskey, G. Koeckelberghs, K. Clays, and M. G. Kuzyk, "Spectroscopic studies of the mechanism of reversible photodegradation of 1-substituted aminoanthraquinone-doped polymers," J. Chem. Phys. **144**, 114902 (2016).
[28] P. Dhakal and M. G. Kuzyk, "Molecular structure and reversible photodegradation in anthraquinone dyes," J. Photochem. and Photobiol. A **328**, 66–76 (2016).
[29] P. Dhakal and M. G. Kuzyk, "Self-Healing Properties of 1-Amino,2,4-Dibromoanthraquinone Dye Doped in PMMA Polymer," J. Phys. Chem. C **121**, 351–360 (2017).
[30] N. Stubbs, M. Bridgewater, M. Stubbs, M. Crescimanno, M. G. Kuzyk, and N. J. Dawson, "Polylactic acid promotes healing of photodegraded disperse orange 11 molecules," Opt. Mater. **76**, 11–15 (2018).
[31] S. K. Ramini and M. G. Kuzyk, "A self healing model based on polymer-mediated chromophore correlations," J. Chem. Phys. **137**, 054705 (2012).
[32] B. Anderson and M. G. Kuzyk, "Generalizing the correlated chromophore domain model of reversible photodegradation to include the effects of an applied electric field," Phys. Rev. E **89**, 032601 (2014).
[33] B. R. Anderson, R. Gunawidjaja, and H. Eilers, "Self-healing organic-dye-based random lasers," Opt. Lett. **40**, 577–580 (2015).
[34] B. R. Anderson, R. Gunawidjaja, and H. Eilers, "Photodegradation and self-healing in a rhodamine 6g dye and y_2o_3 nanoparticle-doped polyurethane random laser," Appl. Phys. B **120**, 1–12 (2015).
[35] B. R. Anderson, R. Gunawidjaja, and H. Eilers, "Random lasing and reversible photodegradation in disperse orange 11 dye-doped pmma with dispersed zro_2 nanoparticles," J. Opt. **18**, 015403 (2016).
[36] N. D. Christianson, Y. Lu, and N. J. Dawson, "Recovery of photodegraded rhodamine 6g in ester-containing polymer matrices," Photochem. Photobiol. Sci. **18**, 2865–2874 (2019).
[37] T. Kazmierczak, H. Song, A. Hiltner, and E. Baer, "Polymeric One-Dimensional Photonic Crystals by Continuous Coextrusion," Macromol. Rapid Commun. **28**, 2210–2216 (2007).
[38] R. Zondervan, F. Kulzer, M. A. Kolchenko, and M. Orrit, "Photobleaching of Rhodamine 6g in Poly(vinyl alcohol) at the Ensemble and Single-Molecule Levels," J. Phys. Chem. A **108**, 1657–1665 (2004).